nature chemistry

ARTICLES

PUBLISHED ONLINE: 5 DECEMBER 2016 | DOI: 10.1038/NCHEM.2665

Dynamics of the triplet-pair state reveals the likely coexistence of coherent and incoherent singlet fission in crystalline hexacene

Nicholas R. Monahan[1], Dezheng Sun[2], Hiroyuki Tamura[3], Kristopher W. Williams[1], Bolei Xu[4], Yu Zhong[1], Bharat Kumar[1], Colin Nuckolls[1], Avetik R. Harutyunyan[5], Gugang Chen[5], Hai-Lung Dai[4], David Beljonne[6]*, Yi Rao[4]* and X.-Y. Zhu[1]*

The absorption of a photon usually creates a singlet exciton (S_1) in molecular systems, but in some cases S_1 may split into two triplets ($2\times T_1$) in a process called singlet fission. Singlet fission is believed to proceed through the correlated triplet-pair ^{1}(TT) state. Here, we probe the ^{1}(TT) state in crystalline hexacene using time-resolved photoemission and transient absorption spectroscopies. We find a distinctive ^{1}(TT) state, which decays to $2\times T_1$ with a time constant of 270 fs. However, the decay of S_1 and the formation of ^{1}(TT) occur on different timescales of 180 fs and <50 fs, respectively. Theoretical analysis suggests that, in addition to an incoherent $S_1 \rightarrow {}^1$(TT) rate process responsible for the 180 fs timescale, S_1 may couple coherently to a vibronically excited ^{1}(TT) on ultrafast timescales (<50 fs). The coexistence of coherent and incoherent singlet fission may also reconcile different experimental observations in other acenes.

The potential for singlet fission to increase the power conversion efficiency of solar cells[1] has motivated significant research effort. The prevalent model for singlet fission dates back to the discovery of the phenomenon approximately 50 years ago and involves the formation of two distinct triplets from an intermediate ^{1}(TT), often called a correlated triplet-pair state[2,3]. This mechanism is described in a two-molecule picture as

$$S_0 + S_1 \leftrightarrows {}^1(TT) \leftrightarrows 2T_1 \quad (1)$$

where S_0 is the ground state, S_1 is the singlet excited state and T_1 is the triplet excited state. The correlated triplet pair, ^{1}(TT), has singlet spin and double-excitation character and may be called a multi-exciton or biexciton state[4]. This model was proposed by Merrifield and Johnson[5] and elaborated by Suna[6]. Smith and Michl[2,3] carried out extensive analysis and pointed out that the rate of singlet fission is the rate for the formation of $2T_1$, not that of ^{1}(TT). Here, the two triplets in $2T_1$ have lost electronic coherence, but can remain spin-coherent for much longer times.

Within the model described by equation (1), ^{1}(TT) is formed incoherently from S_1, a state that is usually synonymous with the molecularly localized Frenkel exciton (FE) but may contain substantial charge transfer (CT) character in crystalline organic semiconductors[7–9]. In contrast, Greyson *et al.*[10] proposed that S_1 and ^{1}(TT) can form quantum coherently, particularly in the presence of CT-mediated electronic coupling. The quantum coherent model has found support from the experiments of Zhu and co-workers, who observed the nearly simultaneous formation of ^{1}(TT) and S_1 in time-resolved two-photon photoemission (TR-2PPE) spectroscopy of polycrystalline pentacene[11] and tetracene[12]. The electronic coupling between S_1 and ^{1}(TT) mediated by the CT components may allow ^{1}(TT) to borrow oscillator strength from the optically bright FE state[8,13,14], and the broad electronic and excitonic bandwidths expected in crystalline organic semiconductors[15–17] may aid in meeting the energy resonant condition[18]. A recent analysis of magnetic dipoles also suggested the delocalized band nature of the ^{1}(TT) state in crystalline tetracene[19].

The nature of the ^{1}(TT) state has been under debate recently. Some believed that there was little difference between ^{1}(TT) and $2T_1$ and proposed a single electronic state, TT, which is formed from S_1 through a non-adiabatic or adiabatic transition[20,21]. The absence of a distinct ^{1}(TT) state seems to be in conflict with the quantum coherent model[10–13], but a recent two-dimensional photon echo study[22] supported the quantum coherent model and showed that the coupling is of mixed electronic–vibrational character (that is, vibronic).

To address the existence of a distinct ^{1}(TT) state during singlet fission, we investigate crystalline hexacene. We chose crystalline hexacene, because singlet fission is highly exoergic and ^{1}(TT) should be energetically well separated from S_1 and T_1. S_1 resides 1.48 eV above S_0 (ref. 23). A theoretical prediction[24] puts T_1 at 0.46 eV above S_0 in the gas phase. The triplet pair is expected at ≥0.56 eV below S_1. Transient absorption (TA) studies on polycrystalline hexacene and derivatized hexacene reported singlet fission timescales of ~0.5 ps (ref. 25) and ~5 ps (ref. 26), respectively.

We probed singlet fission in crystalline hexacene using two complementary techniques: TR-2PPE and TA spectroscopies. The energy resolution of TR-2PPE allowed us to detect a distinctive ^{1}(TT) state at 0.59 eV below S_1. TR-2PPE also revealed that the decay of S_1 and the formation of ^{1}(TT) occur on different timescales of 180 fs and 45 fs, respectively. TA spectroscopy confirmed the appearance of a triplet-like spectral signature on the ultrafast timescale of <50 fs. Rate equation calculations and quantum dynamics simulations suggest that an incoherent $S_1 \rightarrow {}^1$(TT) rate process is

[1]Department of Chemistry, Columbia University, New York, New York 10027, USA. [2]Department of Physics, Columbia University, New York, New York 10027, USA. [3]Advanced Institute for Materials Research, Tohoku University, Sendai 980-8577, Japan. [4]Department of Chemistry, Temple University, Philadelphia, Pennsylvania 19122, USA. [5]Honda Research Institute USA, Columbus, Ohio 43212, USA. [6]Chimie des Matériaux Nouveaux, Université de Mons, B-7000 Mons, Belgium. *e-mail: xyzhu@columbia.edu; yirao@temple.edu; david.beljonne@umons.ac.be

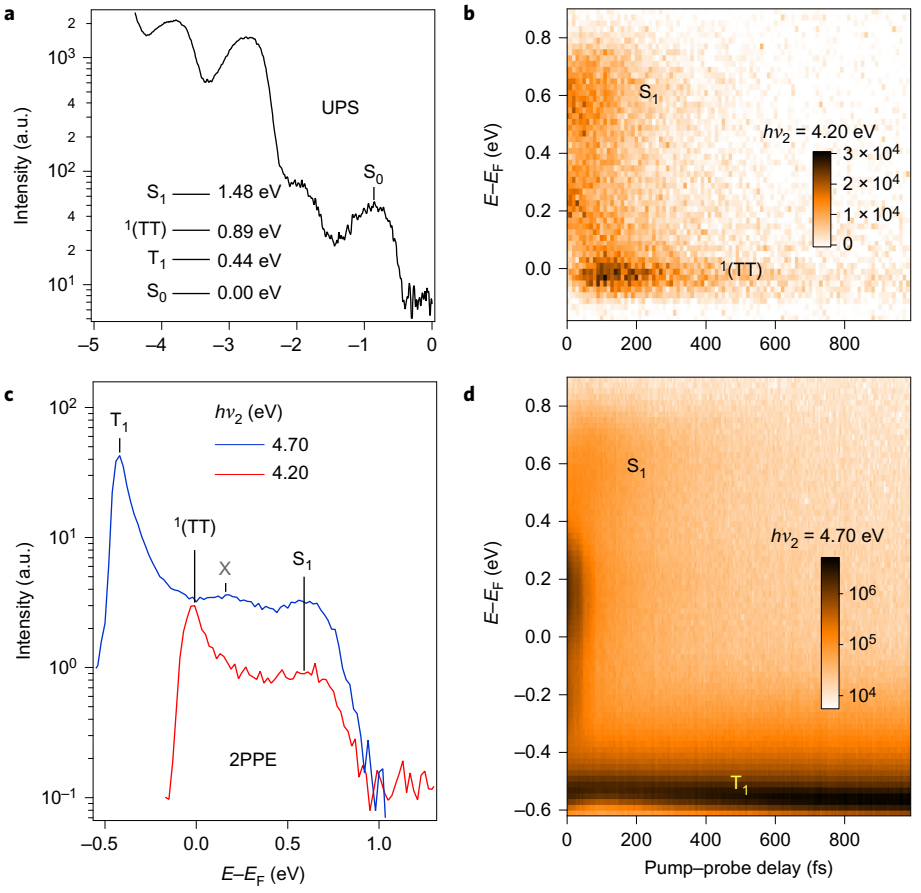

Figure 1 | TR-2PPE and UPS determine quantitatively the energetic positions of S_1, ^{1}(TT) and T_1 above S_0. a, UPS spectrum ($h\nu = 21.22$ eV) of a 10-nm-thick hexacene film deposited on Si(111). The energy scale is referenced to the vacuum level and the S_0 or HOMO peak is labelled. Inset: an energy-level diagram of all excitonic states referenced to S_0. **b**, Pseudo-colour plot of TR-2PPE spectra collected with $h\nu_1 = 1.48$ eV and $h\nu_2 = 4.20$ eV. **c**, 2PPE spectra obtained at a pump–probe delay of $\Delta t = 175$ fs with $h\nu_1 = 1.48$ eV and $h\nu_2 = 4.20$ (red) or 4.70 eV (blue), respectively. **d**, Pseudo-colour plot of TR-2PPE spectra collected with $h\nu_1 = 1.48$ eV and $h\nu_2 = 4.70$ eV. Note that, near-zero pump–probe delay in **b** and **d**, there is a contribution to the 2PPE signal by surface charge-transfer excitons[28] resulting from the ultraviolet pump and near-infrared probe at $\Delta t \leq 0$ fs. The pump and probe laser pulse energy densities are 6 and 0.6 μJ cm^{-2}, respectively.

responsible for the 180 fs S_1 decay time, but the vertically excited S_1 may also coherently couple to a vibronically excited ^{1}(TT) on ultrafast timescales (<50 fs). These results suggest the coexistence of coherent singlet fission from the initial S_1 with more vertical and delocalized character and incoherent singlet fission at long times from a more relaxed and localized S_1.

Results and discussion

In the first experiment, we used polycrystalline hexacene thin films (~10 nm thick) vapour-deposited on a bare Si(111) surface in ultra-high vacuum (UHV). Figure 1a shows the valence band structure revealed by ultraviolet photoemission spectroscopy (UPS). Here, the ionization energy of S_0, located at -0.90 ± 0.05 eV (referenced to the Fermi level), represents the position of the highest occupied molecular orbital (HOMO). Also shown by UPS are HOMO-n ($n = 1, 2,\ldots$) peaks similar to those in pentacene (Supplementary Fig. 1).

We focus on excitons probed in TR-2PPE. This is a pump–probe technique where a pump pulse ($h\nu_1$) creates a transient population of excitonic states that are subsequently ionized by a second pulse ($h\nu_2$), with electrons detected by an energy analyser[11,12]. The electron kinetic energy gives the ionization potential of each state[27]. The laser system consists of two home-built noncollinear optical parametric amplifiers (NOPAs) pumped by a Yb-doped fibre laser (Clark-MXR Impulse)[28]. This allows independent tuning of $h\nu_1$ and $h\nu_2$, with cross-correlation (CC) of the two pulses characterized by a full-width at half-maximum (FWHM) of 99 ± 5 fs. We fix $h\nu_1$ at 1.48 eV, which is the lowest $S_0 \rightarrow S_1$ transition energy[23] and tune $h\nu_2$ to reach resonant conditions for the ionization of each excitonic state (Supplementary Fig. 2).

Figure 1b presents a pseudo-colour (intensity) representation of TR-2PPE spectra as a function of pump–probe delay (Δt), obtained with $h\nu_2 = 4.20$ eV. We observe the short-lived S_1 peak at 0.58 ± 0.05 eV, which is at the expected 1.48 eV above S_0, and a transient peak at -0.01 ± 0.05 eV, that is, 0.59 ± 0.05 eV below S_1, assigned to ^{1}(TT) as it is at the position of the triplet pair. The ^{1}(TT) peak intensity decreases when we tune $h\nu_2$ away from the resonant condition, as illustrated in Fig. 1d for $h\nu_2 = 4.70$ eV. At this $h\nu_2$, the 1(TT) peak merges into a broad distribution, but CC analysis at the position for ^{1}(TT) shows the same kinetic profile as that from the well-resolved ^{1}(TT) in Fig. 1a (Supplementary Fig. 3). The higher photon energy permits the ionization of the long-lived T_1 state located at 0.44 ± 0.05 eV above S_0. Note that, due to the high repetition rate (1 MHz) of the laser, there is a steady-state accumulation of long-lived T_1 states that give rise to a photo-ionization signal at negative Δt (Supplementary Fig. 4). Figure 1c shows representative 2PPE spectra at a pump–probe delay of $\Delta t = 175$ fs for two ionization photon energies: $h\nu_2 = 4.20$ and 4.70 eV. At $h\nu_2 = 4.70$ eV, we also observe a peak (labelled 'X') at ~0.44 eV below S_1. The position of this peak differs from that of S_1 by the energy of T_1 and shows dynamics identical to those of S_1. It is

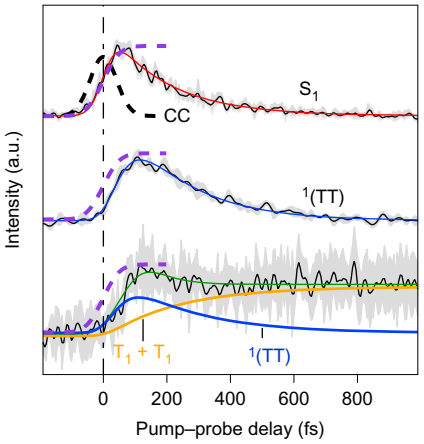

Figure 2 | A comparison of experimental cross-correlations and associated fits for S_1, ^{1}(TT) and T_1. The solid black curves are mean experimental data and the grey shading represents standard deviation. The experimental curves are from TR-2PPE spectra with different $h\nu_2$ and integrated across a small energy window (0.1 eV) within the spectra where each state is best resolved. The solid coloured lines are kinetic fits as detailed in the text. The black dashed curve is the laser pump–probe cross-correlation (CC, FWHM = 99 ± 5 fs), and the purple-curves (reproduced on each kinetic profile) are the time integrations of the CC that represent the predicted rise in population that would be expected due to direct optical excitation.

assigned to the second ionization potential of S_1 with predominantly CT character, as suggested by Yost *et al.*[20] (Supplementary Fig. 5). The inset in Fig. 1a summarizes the energetic positions of S_0, T_1, ^{1}(TT) and S_1. These results show that there is little binding energy (≤0.01 eV) for the two triplets in crystalline hexacene.

We also examined the dynamics of S_1, ^{1}(TT) and T_1 states from TR-2PPE. The experimental CCs for the three states are presented in Fig. 2. The black dashed curve is the Gaussian CC of the pump and probe pulses. The purple curve (reproduced for each state) is a time-integration of CC and represents the expected rise of a population directly formed from photo-excitation. A comparison of the purple curves to the experimental data shows that S_1 is formed by optical excitation, but there is a delay in forming ^{1}(TT) or T_1. Functional fits to the data are shown as solid coloured curves. The S_1 signal is well described by a convolution of CC and an exponential decay with time constant $\tau^{d}_{S_1} = 180 \pm 10$ fs. We fit the ^{1}(TT) profile with a convolution of CC and two exponentials: a rise with time constant of $\tau^{f}_{TT} = 45 \pm 20$ fs and a decay with $\tau^{d}_{TT} = 270 \pm 10$ fs. The ^{1}(TT) state possesses both singlet and triplet-pair characteristics. For the latter, photo-ionization leaves behind a T_1 state, plus a hole in the HOMO; this results in an electron kinetic energy equal to that of the T_1 state[11]. Because the decay of ^{1}(TT) is expected to give 2×T_1, the TR-2PPE kinetic profile at the T_1 energy can be described by a linear sum of contributions from ^{1}(TT) (blue curve) and T_1 (orange curve) from the decay of ^{1}(TT) with a time constant of $\tau^{d}_{TT} = 270 \pm 10$ fs.

To further understand the ^{1}(TT) state, we carried out a TA study on hexacene single crystals (1.2 μm thickness). Optical transition cross-sections are highly anisotropic not only for the $S_0 \rightarrow S_1$ transition[25], but also for transitions from excited states, as demonstrated by Kolata *et al.*[29] in the identification of the promptly formed ^{1}(TT) state in perfluoropentacene. Here, the $h\nu_1 = 1.55$ eV pump pulse and the white light probe pulse were focused onto the sample through a ×10 microscope objective with the polarizations of both beams parallel to the *b* crystalline direction, which is defined as the one having the lowest energy resonance in the absorption spectrum[25].

Figure 3a,b presents two-dimensional pseudo colour plots of TA spectra as functions of probe photon energy and pump–probe delay (Δt) for a pump pulse energy density of $p = 0.90$ mJ cm^{-2}. Photo-excitation results in ground-state bleaching (GB) peaked at 1.74 and 1.89 eV, respectively[25]; the threshold bleaching peak at ~1.48 eV is outside this probe window. The excited state absorption (EA) (Fig. 3b), features two long-lived EA peaks, T_1 (a) and T_1 (b) at 2.05 and at 2.25 eV, respectively, assigned to the $T_1 \rightarrow T_n$ transitions[25,30,31], and a broad, short-lived peak in the range of ~2.15–2.45 eV. The latter has been assigned by Busby *et al.*[25] as the EA of the S_1 state, which overlaps with T_1 (b). The most striking result from Fig. 3b is that the two EA peaks assigned to T_1 rise concurrently with that of S_1, as well as the GB of S_0 in Fig. 3a. To further illustrate this, Fig. 3c presents spectra of the EA region at selected pump–probe delays (Δt). Except for the extra intensity under the broad peak in the range of ~2.15–2.45 eV attributed to S_1 at the shortest time ($\Delta t = 0.06$ ps), the spectral shape remains nearly constant in the entire time window ($\Delta t = 0.06$–2.5 ps), thus confirming the presence of a T_1-like EA signal formed within the experimental time resolution (±50 fs), as determined by the pump–probe cross correlation (blue curve in Fig. 3d).

Figure 3d presents kinetic profiles at 1.74 and 1.89 eV for the GB spectral region. The ultrafast rises in $\Delta T/T$ due to photo-excitation are followed by a slight decay in the time window shown here. Kinetic fits are based on a convolution of the laser CC curve (blue curve) and an apparent decay time constant of 30 ± 10 ps. The decay probably results from T_1–T_1 annihilation at the high excitation density, as confirmed at a lower pump pulse energy density of $p = 0.15$ mJ cm^{-2} where decay was negligible (Supplementary Fig. 6a). Note that triplet decay due to annihilation is a second-order process, which may be probed on longer timescales. We restricted our focus to the short time dynamics presented here.

Figure 3e shows kinetic profiles in the EA spectra region: $h\nu_2 = 2.05$ eV for T_1 (a) and $h\nu_2 = 2.25$ and 2.39 eV for T_1 (b). All kinetic profiles are characterized by rises in EA ($-\Delta T/T$) within the experimental time resolution. Thus, we conclude that a T_1-like state is formed on ultrafast timescales (≤50 fs). Beyond the ultrafast rise, the kinetic profiles of the two T_1 EA peaks differ on a longer timescale. For T_1 (b), probing at 2.25 and 2.36 eV shows similar profiles, each well-described by kinetic fits consisting of a fast decay of $\tau^{d}_{1} = 180 \pm 30$ fs, followed by the slow decay with a time constant of $\tau_A = 30 \pm 10$ ps attributed to T_1–T_1 annihilation. Here, the fast decay comes from the short-lived and overlapping S_1 peak and τ^{d}_{1} is the same as the S_1 decay time of $\tau^{d}_{S_1} = 180 \pm 10$ fs seen in TR-2PPE. The kinetic profile of the isolated T_1 (a) at 2.05 eV is well described by an ultrafast rise within the experimental time resolution, followed by a nearly steady-state signal in the probe time window. The absence of slow decay attributed to T_1–T_1 annihilation at this probe photon energy is due to a rise in the T_1 population, as is obvious at lower excitation densities (Supplementary Fig. 6b).

Before presenting a unified view on singlet fission in hexacene, we must point out a common misconception in representing the time-dependent population of a state by the time-dependent change in spectroscopic signal. In reality, the signal in conventional spectroscopy is proportional to the product of population ρ and transition cross-section σ. Here, the optical transitions in TA for the ^{1}(TT), isolated T_1 and S_1 states are given by

$$^1(T_1T_1) \xrightarrow{\sigma_2} {}^1(T_1T_n) \quad (2)$$

$$T_1 \xrightarrow{\sigma_3} T_n \quad (3)$$

$$S_1 \xrightarrow{\sigma_4} S_n \quad (4)$$

We note that, although both equations (2) and (3) contribute to the $T_1 \rightarrow T_n$ signal in transient absorption, they may have different transition cross-sections and time-dependent populations.

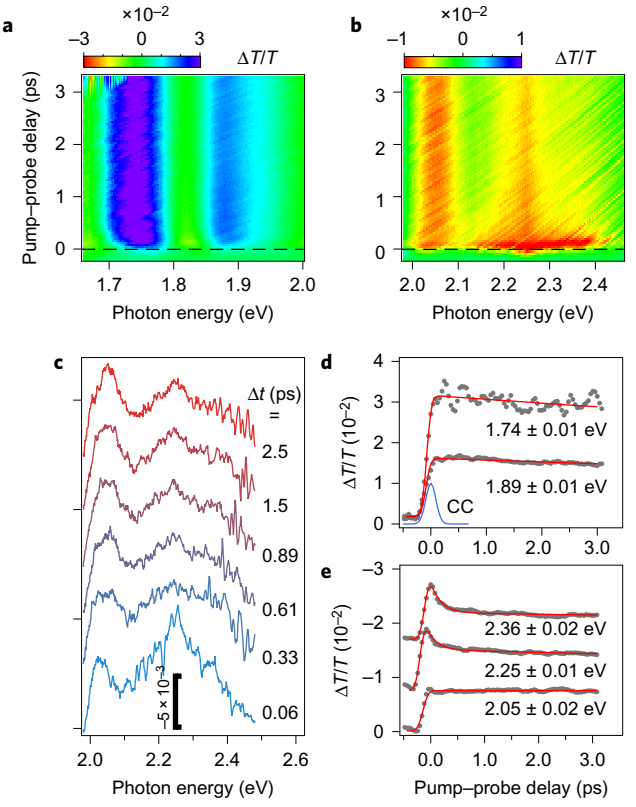

Figure 3 | Transient absorption spectroscopy reveals the ultrafast appearance of a triplet-like signature. a,**b**, Two-dimensional pseudo-colour plots of TA spectra from single-crystal hexacene excited at 1.55 eV and with the probe white light polarized along the *b* crystalline axis. Note the different colour scales for the ground-state bleaching in **a** and excited-state absorption in **b**. **c**, TA spectra at the indicated pump–probe delays. **d**,**e**, Kinetic profiles obtained from vertical cuts in **a** and **b**, respectively. In each case, the data points were averaged over the indicated probe photon energy range (±0.01 or ±0.02 eV). Red curves are kinetic fits as detailed in the text. The blue curve in **d** is the laser pump–probe CC. The pump laser pulse energy density is 0.9 mJ cm^{-2}.

The two transitions in TR-2PPE of the ^{1}(TT) state are represented as

$$^1(T_1T_1) \xrightarrow{\sigma_{5a}} h^+ + e^- \quad (5a)$$

$$^1(T_1T_1) \xrightarrow{\sigma_{5b}} T_1 + h^+ + e^- \quad (5b)$$

where expression (5a) reveals the singlet character and expression (5b) the triplet-pair character of the ^{1}(TT) state. The latter leaves behind T_1 as a final state. The transitions from an isolated T_1 and an S_1 of FE and/or CT character are given by

$$T_1 \xrightarrow{\sigma_6} h^+ + e^- \quad (6)$$

$$S_1 \xrightarrow{\sigma_7} h^+ + e^- \quad (7)$$

In TR-2PPE, h^+ represents a hole in the HOMO and e^- a final molecular resonance above the vacuum level or a free electron state (Supplementary Fig. 2).

Both TR-2PPE and TA measurements show the optical excitation of the S_1 state, which decays with a time constant of $\tau^d_{S_1} = 180$ fs. We observe the distinct ^{1}(TT) peak in 2PPE with a rise time constant of 45 ± 20 fs and T_1-like absorption in TA within 50 fs. This initial ^{1}(TT) state is probably an excited ^{1}(TT)*, given the 0.59 eV energy difference between S_1 and the triplet pair. The excess excitation energy in ^{1}(TT)* is probably vibronic in nature, as suggested by Bakulin *et al.*[22] for singlet fission in pentacene derivatives. TR-2PPE (Fig. 1b) and TA (Fig. 3c) show little change in peak position within the lifetime of the excited ^{1}(TT)* state. One possible interpretation is that similarities in the geometries of intermediate and final states in the probe step may leave much of the excess vibrational energy in the final state. There is also limited time resolution: as shown in the following, a quantum dynamics simulation reveals ultrafast loss of the vibrational energy in the mode of interest to the phonon bath and we may not have sufficient time resolution to resolve this process.

Energy-resolved TR-2PPE measurements show the clear decay of the ^{1}(TT) state with a time constant of $\tau^d_{TT} = 270 \pm 10$ fs, leading to an additional T_1 signal with the same rise time, $\tau^f_{T_1} = 280 \pm 30$ fs (Supplementary Fig. 6). The two EA peaks at ~2.05 and ~2.25 eV probe not only the triplet-pair character of the ^{1}(TT) state but also the isolated T_1 states. The relative cross-sections for the $T_1 \rightarrow T_n$ transition from ^{1}(TT) (σ_2) and T_1 (σ_3) can be different, as is evident from the different kinetic profiles for T_1 (a) and T_1 (b) in Fig. 3d,e. The TA data in Fig. 3 are obtained with probe light polarization along the *b* crystalline direction. For polarization along the *a* direction (Supplementary Fig. 7), we find that σ_3 is larger than σ_2. As a result, the kinetic profile for the T_1 (a) EA peak shows the slow rising T_1 signal with an amplitude ~1.5 times that of the ultrafast ^{1}(TT) signal. Interestingly, the slow rise component shows an apparent time constant of 700 ± 50 fs along *a*, which is 2.5 times the 280 fs time constant along *b*. An average of these apparent time constants accounts for the 530 fs singlet fission time observed in TA from polycrystalline samples[25]. Polarization and crystalline angle-dependent transient absorption has been observed before for singlet fission in perfluoropentacene[29] or tetracene[32,33]. In the time window of ~280–700 fs for hexacene probed here, the most likely transient species are correlated triplet pairs (equation (2)) and isolated triplets (equation (3)), and the EA signal along the *b* direction may contain a greater contribution from the former than that along the *a* direction.

The main puzzle from the experimental findings is the distinctively different timescales: S_1 decays with $\tau^d_{S_1} = 180$ fs, while ^{1}(TT) is formed with $\tau^f_{TT} < 50$ fs and decays to $2\times T_1$ with $\tau^d_{TT} = 270 \pm 10$ fs. Neither a coherent superposition mechanism nor an incoherent rate process alone can explain the three timescales. To understand singlet fission in hexacene, we carried out incoherent rate and coherent quantum dynamics calculations.

We start by considering incoherent singlet fission from S_1, which is expected to occur in the inverted Marcus regime. In ref. 25, a multiphonon relaxation theory was applied to acenes and predicted an singlet fission time of ~2 ps in hexacene. A refined model treats these interactions exactly in the framework of the Fermi golden rule and, as done here, its Marcus–Levich–Jortner formulation[34], which accounts for coupling to classical low-frequency phonons and for quantum-mechanical tunnelling via a dominant high-frequency vibrational mode (as usual, the stretching/breathing mode at 1,450 cm^{-1})[25]. When using essentially the same parameters as in ref. 25 (electronic coupling of 30 meV, internal and external reorganization energies of 250 and 100 meV, respectively), we obtain an SF time constant of ~160 fs for a driving force, $\Delta E_{SF} = 2E(T_1) - E(S_1)$, of −0.59 eV, in excellent agreement with the measured $\tau^d_{S_1}$. The corresponding values for $\Delta E_{SF} = -0.11$ eV and 0.11 eV in pentacene and tetracene are 80 fs and ~10 ps, respectively (Fig. 4a), in agreement with experimental data[11,20,35–37]. Despite the success in predicting the S_1 decay rates, the incoherent model cannot account for the much faster formation (<50 fs) of ^{1}(TT) states observed in experiments. To overcome this limitation, we turn to a coherent model and a quantum dynamics calculation (for details see Supplementary Information, pages 8–9).

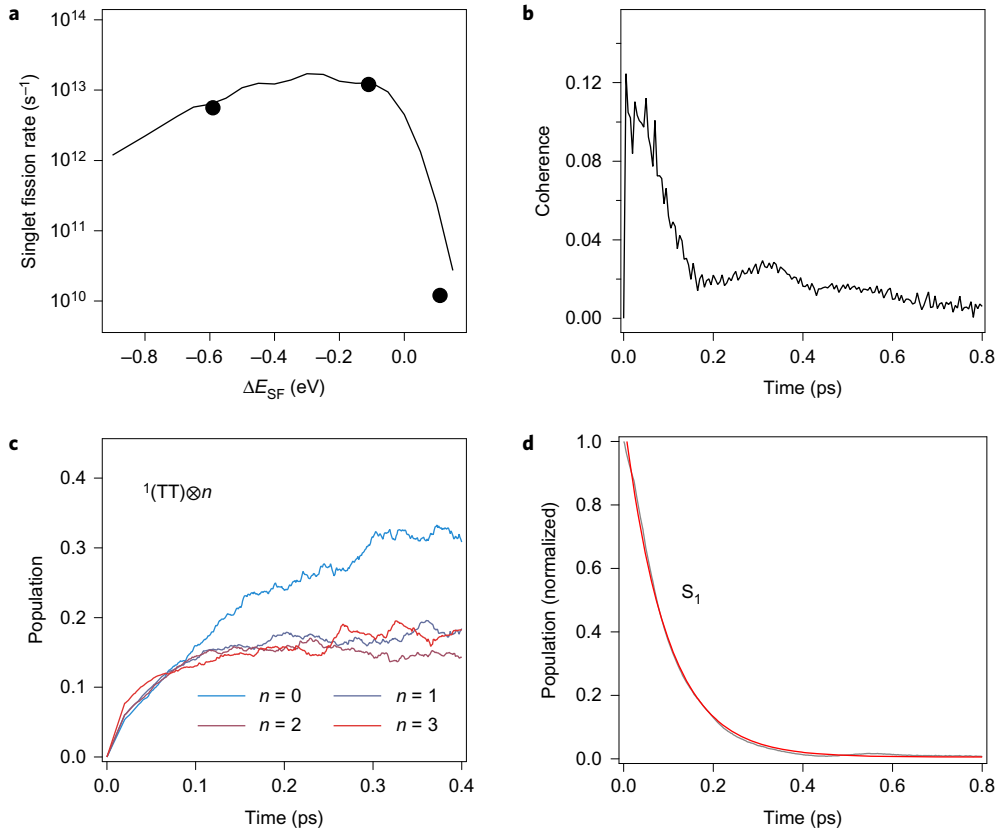

Figure 4 | Incoherent and coherent rates from theoretical calculations and simultions. a, Incoherent singlet fission rate as a function of energy driving force in acenes from Marcus–Levich–Jortner electron transfer theory (black circles correspond to experimental data). **b**, S_1–^{1}(TT)⊗3 coherence, which is particularly large for the first 100 fs. **c**, Relative (integrated to one) TT⊗*n* populations as a function of time. Note that the ^{1}(TT)⊗3 state is formed first, with a single-exponential rise time of 40 ± 10 fs. **d**, S_1 population (grey) as a function of time. The red curve is a single exponential fit (red) with a time constant of 100 fs. The initial conditions correspond to excitation of S_1.

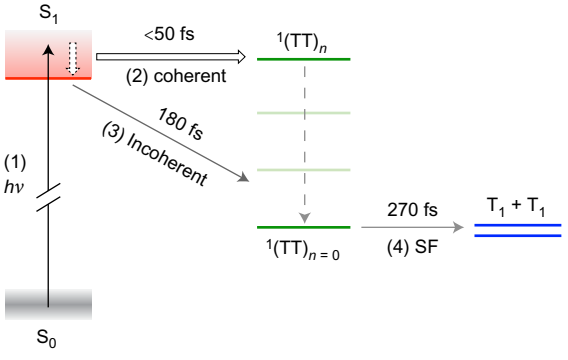

Figure 5 | Summary of singlet fission mechanism in crystalline hexacene. Red: S_1 state. Green: vibrational manifold of ^{1}(TT). Blue: two individual triplets. There can be a coexistence of coherent and incoherent singlet fission. The initial S_1 with more vertical and delocalized character can coherently couple to a vibronically excited ^{1}(TT) on ultrafast timescales (<50 fs) and a more relaxed and localized S_1 may undergo an incoherent $S_1 \rightarrow {}^1$(TT) rate process with the 180 fs time constant. The ^{1}(TT) state separates into two triplets on a timescale of 270 fs.

The experimental timescale of $\tau_{TT}^{f} < 50$ fs is consistent with the quantum coherent formation of an excited ^{1}(TT)* state, probably vibronic in nature, from S_1. Among a number of possibilities of vibronic coupling, the large ΔE_{SF} in hexacene is, for example, commensurate with three vibrational quanta of the 1,450 cm^{-1} vibrational mode and, for illustrative purposes, we consider coherence involving $S_1 \otimes n = 0$ and ^{1}(TT)⊗$n = 3$ (where the notation $\otimes n = i$ indicates a product state with a vibrational wavefunction in quantum state $n = i$). Because the experimental τ_{TT}^{f} <50 fs is on the order of the vibrational period of $\tau_v = 23$ fs (for the 1,450 cm^{-1} mode), we suggest that the crossing point between the S_1 and the ^{1}(TT) potential energy surfaces is probably close to or within the Franck–Condon region for the initial optical excitation, $S_0 \rightarrow S_1$ (Supplementary Fig. 8). In this scenario, vibrational wavepacket motion from the initial Franck–Condon region to the formation of S_1 and ^{1}(TT)⊗$n = 3$ superposition can occur on the ultrafast timescale of τ_v. To understand the vibronic coherence, we perform quantum dynamics simulations for a model two-electronic state system using the multi-configurational time-dependent Hartree (MCTDH) method[38,39]. Here, we explicitly include 30 high-frequency and 18 low-frequency vibration modes, out of which we construct one effective mode[40] at 1,450 cm^{-1} and a set of bath modes. The electronic coupling (30 meV) and the reorganization energies for the high-frequency (240 meV) and low-frequency vibrations (30 meV) are comparable to those used in the Marcus–Levich–Jortner rate calculations above. The MCTDH calculations show that the initially prepared $S_1 \otimes n = 0$ Franck–Condon state quickly evolves into a coherent superposition (Fig. 4b) with the resonant ^{1}(TT)⊗$n = 3$ state. The build-up of the vibronic coherence is accompanied by a small population transfer to the triplet-pair states, mostly ^{1}(TT)⊗$n = 3$ with a rise time of 40 ± 10 fs (Fig. 4c), in excellent agreement with experiment and followed by vibrational redistribution among the $n = 0$, 1, 2, 3 states. Such ultrashort time scales for vibrational energy redistribution are known for poly-atomic molecules in the condensed phase[41].

On a longer timescale, we see dephasing and population conversion from S_1 (blue) to $^1(TT)$ (red) with a time constant of ~100 fs, which is slightly shorter than that of the incoherent rate calculation.

We propose the following mechanism for singlet fission in crystalline hexacene (Fig. 5). (1) Initial photon absorption (black arrow) excites the vertical and delocalized S_1 state, which (2) evolves into vibronic coherence with $^1(TT)_n$ on an ultrafast timescale (≤50 fs) and then dephases. (3) Concurrent with step (2), the vertical and delocalized S_1 state relaxes (hollow arrow) to a more adiabatic and localized S_1, which undergoes an incoherent rate process with a characteristic timescale of 180 fs to form $^1(TT)_n$. The $^1(TT)_n$ resulting from either steps (2) and (3) can undergo vibrational redistribution and relaxation (dashed arrow). (4) The $^1(TT)$ separates into two triplets—that is, singlet fission—with a characteristic time constant of 270 fs. Note that on much longer timescales (ns), the two triplets can remain spin-coherent[19,42]. The proposed mechanisms may also reconcile differences in the literature on singlet fission mechanisms in pentacene and tetracene. Thus, the two prevailing proposals for crystalline acenes, quantum coherent[8,11–14] or incoherent[20,21,35,37], may each have revealed part of this singlet fission mechanism.

Received 16 March 2016; accepted 3 October 2016;
published online 5 December 2016

References

1. Hanna, M. C. & Nozik, A. J. Solar conversion efficiency of photovoltaic and photoelectrolysis cells with carrier multiplication absorbers. *J. Appl. Phys.* **100,** 074510 (2006).
2. Smith, M. B. & Michl, J. Singlet fission. *Chem. Rev.* **110,** 6891–6936 (2010).
3. Smith, M. B. & Michl, J. Recent advances in singlet fission. *Annu. Rev. Phys. Chem.* **64,** 361–386 (2013).
4. Trinh, M. T. et al. Intra- to intermolecular singlet fission. *J. Phys. Chem. C* **119,** 1312–1319 (2015).
5. Johnson, R. C. & Merrifield, R. E. Effects of magnetic fields on the mutual annihilation of triplet excitons in anthracene crystals. *Phys. Rev. B* **1,** 896–902 (1970).
6. Suna, A. Kinematics of exciton–exciton annihilation in molecular crystals. *Phys. Rev. B* **1,** 1716–1739 (1970).
7. Yamagata, H. *et al.* The nature of singlet excitons in oligoacene molecular crystals. *J. Chem. Phys.* **134,** 204703 (2011).
8. Beljonne, D., Yamagata, H., Brédas, J. L., Spano, F. C. & Olivier, Y. Charge-transfer excitations steer the Davydov splitting and mediate singlet exciton fission in pentacene. *Phys. Rev. Lett.* **110,** 226402 (2013).
9. Sharifzadeh, S., Darancet, P., Kronik, L. & Neaton, J. B. Low-energy charge-transfer excitons in organic solids from first-principles: the case of pentacene. *J. Phys. Chem. Lett.* **4,** 2197–2201 (2013).
10. Greyson, E. C., Vura-Weis, J., Michl, J. & Ratner, M. A. Maximizing singlet fission in organic dimers: theoretical investigation of triplet yield in the regime of localized excitation and fast coherent electron transfer. *J. Phys. Chem. B* **114,** 14168–14177 (2010).
11. Chan, W.-L. *et al.* Observing the multiexciton state in singlet fission and ensuing ultrafast multielectron transfer. *Science* **334,** 1541–1545 (2011).
12. Chan, W.-L., Ligges, M. & Zhu, X.-Y. The energy barrier in singlet fission can be overcome through coherent coupling and entropic gain. *Nat. Chem.* **4,** 840–845 (2012).
13. Chan, W.-L. *et al.* The quantum coherent mechanism for singlet fission: experiment and theory. *Acc. Chem. Res.* **46,** 1321–1329 (2013).
14. Aryanpour, K., Dutta, T., Huynh, U. N. V., Vardeny, Z. V. & Mazumdar, S. Theory of primary photoexcitations in donor–acceptor copolymers. **115,** 267401 (2015).
15. Tiago, M., Northrup, J. & Louie, S. *Ab initio* calculation of the electronic and optical properties of solid pentacene. *Phys. Rev. B* **67,** 115212 (2003).
16. Bardeen, C. J. The structure and dynamics of molecular excitons. *Annu. Rev. Phys. Chem.* **65,** 127–148 (2014).
17. Cudazzo, P., Sottile, F., Rubio, A. & Gatti, M. Exciton dispersion in molecular solids. *J. Phys. Condens. Matter* **27,** 113204 (2015).
18. Monahan, N. & Zhu, X.-Y. Charge transfer-mediated singlet fission. *Annu. Rev. Phys. Chem.* **66,** 601–618 (2014).
19. Wang, R. *et al.* Magnetic dipolar interaction between correlated triplets created by singlet fission in tetracene crystals. *Nat. Commun.* **6,** 8602 (2015).
20. Yost, S. R. *et al.* A transferable model for singlet-fission kinetics. *Nat. Chem.* **6,** 492–497 (2014).
21. Musser, A. J. *et al.* Evidence for conical intersection dynamics mediating ultrafast singlet exciton fission. *Nat. Phys.* **11,** 352–357 (2015).
22. Bakulin, A. A., Morgan, S. E., Kehoe, T. B., Wilson, M. W. B. & Chin, A. W. Real-time observation of multiexcitonic states in ultrafast singlet fission using coherent 2D electronic spectroscopy. *Nat. Chem.* **8,** 16–23 (2016).
23. Watanabe, M. *et al.* The synthesis, crystal structure and charge-transport properties of hexacene. *Nat. Chem.* **4,** 574–578 (2012).
24. Houk, K. N., Lee, P. S. & Nendel, M. Polyacene and cyclacene geometries and electronic structures: bond equalization, vanishing band gaps, and triplet ground states contrast with polyacetylene. *J. Org. Chem.* **66,** 5517–5521 (2001).
25. Busby, E. *et al.* Multiphonon relaxation slows singlet fission in crystalline hexacene. *J. Am. Chem. Soc.* **136,** 10654–10660 (2014).
26. Lee, J. *et al.* Singlet exciton fission in a hexacene derivative. *Adv. Mater.* **25,** 1445–1448 (2013).
27. Zhu, X. Y. How to draw energy level diagrams in excitonic solar cells. *J. Phys. Chem. Lett.* **5,** 2283–2288 (2014).
28. Monahan, N. R., Williams, K. W., Kumar, B., Nuckolls, C. & Zhu, X.-Y. Direct observation of entropy-driven electron–hole pair separation at an organic semiconductor interface. *Phys. Rev. Lett.* **114,** 247003 (2015).
29. Kolata, K., Breuer, T., Witte, G. & Chatterjee, S. Molecular packing determines singlet exciton fission in organic semiconductors. *ACS Nano* **8,** 7377–7383 (2014).
30. Angliker, H., Rommel, E. & Wirz, J. Electronic spectra of hexacene in solution (ground state. Triplet state. Dication and dianion). *Chem. Phys. Lett.* **87,** 208–212 (1982).
31. Chakraborty, H. & Shukla, A. Theory of triplet optical absorption in oligoacenes: from naphthalene to heptacene. *J. Chem. Phys.* **141,** 164301 (2014).
32. Zhang, B. *et al.* Polarization-dependent exciton dynamics in tetracene single crystals polarization-dependent exciton dynamics in tetracene single crystals. *J. Chem. Phys.* **141,** 244303 (2014).
33. Wan, Y. *et al.* Cooperative singlet and triplet exciton transport in tetracene crystals visualized by ultrafast microscopy. *Nat. Chem.* **7,** 785–792 (2015).
34. Brédas, J.-L., Beljonne, D., Coropceanu, V. & Cornil, J. Charge-transfer and energy-transfer processes in π-conjugated oligomers and polymers: a molecular picture. *Chem. Rev.* **104,** 4971–5004 (2004).
35. Wilson, M. W. B. *et al.* Ultrafast dynamics of exciton fission in polycrystalline pentacene. *J. Am. Chem. Soc.* **133,** 11830–11833 (2011).
36. Burdett, J. J., Gosztola, D. & Bardeen, C. J. The dependence of singlet exciton relaxation on excitation density and temperature in polycrystalline tetracene thin films: kinetic evidence for a dark intermediate state and implications for singlet fission. *J. Chem. Phys.* **135,** 214508 (2011).
37. Wilson, M. W. B. *et al.* Temperature-independent singlet exciton fission in tetracene. *J. Am. Chem. Soc.* **135,** 16680–16688 (2013).
38. Meyer, H. D., Manthe, U. & Cederbaum, L. S. The multi-configuration time-dependent Hartree approach. *Chem. Phys. Lett.* **165,** 73–78 (1990).
39. Tamura, H., Huix-Rotllant, M., Burghardt, I., Olivier, Y. & Beljonne, D. First-principles quantum dynamics of singlet fission: coherent versus thermally activated mechanisms governed by molecular π stacking. *Phys. Rev. Lett.* **115,** 107401 (2015).
40. Tamura, H., Ramon, J. G. S., Bittner, E. R. & Burghardt, I. Phonon-driven ultrafast exciton dissociation at donor–acceptor polymer heterojunctions. *Phys. Rev. Lett.* **100,** 107402 (2008).
41. Elsaesser, T. & Kaiser, W. Vibrational and vibronic relaxation of large polyatomic molecules in liquids. *Annu. Rev. Phys. Chem.* **42,** 83–107 (1991).
42. Burdett, J. J. & Bardeen, C. J. Quantum beats in crystalline tetracene delayed fluorescence due to triplet pair coherences produced by direct singlet fission. *J. Am. Chem. Soc.* **134,** 8597–8607 (2012).

Acknowledgements

The TR-2PPE experiments and analysis were supported by the US Department of Energy (grant DE-SC0014563) (from 1 July 2015). X.-Y.Z. acknowledges partial support before 30 June 2015 by the US National Science Foundation (grant DMR 1321405). The TA work was supported by the Honda Research Institute, USA. The work in Mons was supported by the Belgian National Fund for Scientific Research (FRS-FNRS). D.B. is an FNRS Research Director. H.T. acknowledges support from an Invited Professor Fellowship, FNRS, Belgium. X.-Y.Z. thanks D. Reichman, T. Van Voorhis, T. Berkelbach, T. Fauster, W.-L. Chan, M. Tuan Trinh and K. Miyata for discussions. Y.R. thanks T.F. Heinz, F.C. Spano, O. Yaffe and Y. Wu for suggestions. H.T. thanks Y. Kurashige for discussions.

Author contributions

N.R.M. and K.W.W. designed and performed the TR-2PPE experiments. D.S., B.X., A.R.H., G.C. and Y.R. designed and performed the TA experiments. H.T. and D.B. carried out computational studies. B.K. and C.N. synthesized the precursor molecule for single-crystalline or polycrystalline thin-film growth. Y.Z. and C.N. grew the single-crystal sample. N.R.M., X.-Y.Z., D.S. and Y.R. analysed the data. X.-Y.Z., N.R.M. and Y.R. wrote the manuscript. X.-Y.Z. supervised the TR-2PPE experiments. Y.R. and H.-L.D. supervised the TA experiments. All authors were involved in the discussion of the results and contributed to the final version of the manuscript.

Additional information

Supplementary information is available in the online version of the paper. Reprints and permissions information is available online at www.nature.com/reprints. Correspondence and requests for materials should be addressed to D.B., Y.R. and X.-Y.Z.

Competing financial interests

The authors declare no competing financial interests.